

Edge Computing Meets Millimeter-wave Enabled VR: Paving the Way to Cutting the Cord

Mohammed S. Elbamby*, Cristina Perfecto†, Mehdi Bennis*, and Klaus Doppler‡

*Centre for Wireless Communications, University of Oulu, Finland.

emails: {mohammed.elbamby,mehdi.bennis}@oulu.fi

†University of the Basque Country (UPV/EHU), Spain. email: cristina.perfecto@ehu.eus

‡Nokia Bell Labs, Sunnyvale, CA, USA. email: klaus.doppler@nokia-bell-labs.com

Abstract—In this paper, a novel proactive computing and mmWave communication for ultra-reliable and low latency wireless virtual reality (VR) is proposed. By leveraging information about users' poses, proactive computing and caching are used to pre-compute and store users' HD video frames to minimize the computing latency. Furthermore, multi-connectivity is exploited to ensure reliable mmWave links to deliver users' requested HD frames. The performance of the proposed approach is validated on a VR network serving an interactive gaming arcade, where dynamic and real-time rendering of HD video frames is needed and impulse actions of different players impact the content to be shown. Simulation results show significant gains of up to 30% reduction in end-to-end delay and 50% in the 90th percentile communication delay.

I. INTRODUCTION

Commercial 5G deployments are not expected to be available before 2020, however the race to showcase a first pre-standard 5G network is on. Hence, all eyes are set on how brand new services that promise to deliver entirely new experiences such as 360-degree immersive virtual reality (VR) will be offered. However multiple technical challenges need to be investigated to deal with the latency-sensitivity and the resource –communications and computing– intensiveness nature of 4K/8K UHD immersive VR wireless streaming and to realize the vision of interconnected VR [1].

To accommodate the extensive use of resource-hungry applications, it is foreseen that a 1000-fold boost will be needed in system capacity (measured in bps/km²). This will be facilitated via an increased bandwidth, higher densification, and improved spectral efficiency. Zooming on the VR requirements, even anticipating the use of 265 HEVC 1:600 video compression rate, a bit rate of up to 1 Gbps [2] would be needed to match the 2x64 million pixel human-eye accuracy. These rates are unrealizable in 4G and challenging in 5G for a disruption-free immersive VR demands. Therefore significant research efforts around VR have focused on reducing bandwidth needs in mobile/wireless VR, thereby shrinking the amount of data processed and transmitted. Many approaches leverage head and eye-gaze tracking to spatially segment 360° frames and deliver in HD only user's field of view (FOV) matching portion [3], [4]. Alternatively [5] considers a foveated 360° transmission where resolution and color depth are gradually reduced from fovea-centralis area to the peripheral FOV.

Latency is critical for VR; the human eye needs to experience accurate and smooth movements with low (<20 ms) motion-to-photon (MTP) latency [4]–[6]. High MTP values send conflicting signals to the Vestibulo-ocular reflex (VOR), and might lead to dizziness or motion sickness. Both computing (image processing or frame rendering) and communication (queuing and over-the-air transmission) delays represent a

major bottleneck in VR systems. Heavy image processing requires high computational power that is often not available in the local head-mounted device (HMD) GPUs. Offloading computing significantly relieves the computing burden at the expense of incurring an additional communication delay in the downlink (DL) delivery of the processed video frames in full resolution. Moreover, to ensure responsiveness and real-time computing through minimal latency, computing servers should be readily available and located close to the end users.

VR demands a perceptible image-quality degradation-free uniform experience. However, temporary outages due to impairments in measured signal to interference plus noise ratio (SINR) are frequent in mobile/wireless environments. In this regard, an ultra-reliable VR service refers to the timely delivery of video frames with high success rate. Provisioning for a higher reliability pays a toll on the use of resources and allocating more resources for a single user could potentially impact the experienced latency of the remaining users.

Leveraging ubiquitous caching and computing at the wireless network edge will radically change the future mobile network architecture, and alleviate the current bottleneck for massive content delivery. Research ideas and network engineering geared toward exploiting communications, caching, and computing (C³) for future content-centric mobile networks are found in [7]–[9]. This paper exploits the C³ paradigm to provide an enhanced wireless VR experience. To that end, it blends together the use of millimeter-wave (mmWave) technology and fog computing. The former seeks to deliver multi-Gbps wireless communication between VR headsets and network access points, with reliability guarantees, and the latter carries out advanced image processing, effectively offloading client displays or game consoles while satisfying stringent latency constraints. The main contribution of this paper is to propose a joint proactive computing and mmWave resource allocation scheme under latency and reliability constraints. Reliability is ensured by leveraging multi-connectivity (MC) to enhance the performance of users under channel variability, whereas proactive computing and user association is optimized to satisfy the latency requirements.

The rest of this paper is organized as follows. Section II describes the system model and problem formulation. The proposed joint computing and matching scheme is introduced in Section III. Section IV analyzes the performance of the proposed framework. Finally, Section V concludes the paper.

II. SYSTEM MODEL

Consider an indoor, open plan, VR gaming arcade of dimensions $L \times W \times H$ m³ where a set \mathcal{A} of A mmWave band access points (mmAP) serves a set \mathcal{U} of U virtual reality

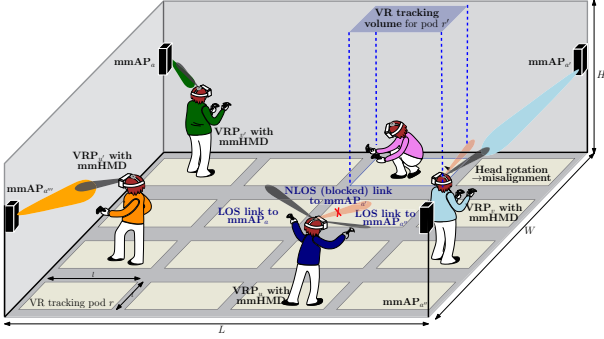


Figure 1. Open-plant VR gaming arcade with VRPs moving freely within their VR tracking pods and getting HD video frames from mmAP.

players (VRP) equipped with wireless mmWave head-mounted VR displays (mmHMD). VRPs are distributed and move freely within the limits of the R individual and $l \times l \text{ m}^2$ sized VR pods such that $R \geq U$. The movement of VRPs in the physical space of each VR pod is tracked and mapped into the virtual space. An illustration of the system model is shown in Fig. 1. The system operates in a time-slotted mode. The time-slots are indexed by $t \in \{1, 2, \dots\}$ with separate scales to account for scheduling decisions, and for beam alignment.

A. Interactive VR Frame Rendering Model

A set \mathcal{I} of impulse actions is defined as the actions generated during the interactive gaming either by the VRPs or an external trigger. The arrival of impulse action $m_i \in \mathcal{I}$ impacts the game play of a subset of VRPs $\mathcal{U}_i \subseteq \mathcal{U}$. In this regard, the impact of the impulse actions on the VRPs' game play, namely, the *impact matrix*, is defined as $\Theta = [\theta_{ui}]$, where $\theta_{ui} = 1$ if $u \in \mathcal{U}_i$, and $\theta_{ui} = 0$ otherwise.¹

Mobile edge computing is used to provide the required computation capabilities. Accordingly, a fog network consisting of a set \mathcal{E} of E edge servers with GPU computing capability c_e , and a storage unit of capacity S HD frames, will perform real-time VR environment building related computing² to generate HD interactive video frames based on the real-time 6D pose³ and the impulse actions of VRPs.

Each VRP u is interested in receiving a unique F -tuple of HD video frames $(V_1^u, V_2^u, \dots, V_F^u)$ throughout its game play. To render an HD video frame, a processing density of κ GPU cycles per bit of frame data is required, with HD frame V_f^u having a data size of L_{fu}^{HD} bits. In this context, mmAPs act as a two-way middleware between the mmHMDs and the edge servers in the fog network. mmAPs relay pose and action inputs from VRPs arriving through the wireless uplink (UL). After the HD frames are rendered, the mmAPs schedule mmWave time slots in the DL to deliver the resulting video frames. To ensure reliable DL transmission, MC is leveraged in which multiple mmAPs can jointly transmit the same data to a player with a weak link. Furthermore, to avoid motion sickness

¹An example of an impulse action is a player firing a gun in a shooting game. As the game play of a subset of players is affected by this action, a computed video frame for any of them needs to be rendered again.

²The terms computing and rendering are used interchangeably throughout the paper to describe the process of rendering HD video frames.

³A 6D pose is jointly given by the 3D location coordinates and the 3 orientation angles over the X, Y, and Z axes, namely the roll, pitch and yaw.

associated with high MTP delay, computing and scheduling decisions have to guarantee stringent latency constraints. Therefore, The fog network leverages the predictability of users' poses to proactively compute the upcoming HD video frames within a prediction window T_w . VRPs can receive and stream the proactively computed video frames as long as they are not affected by impulse actions arriving afterwards. The proactive computing time dynamics are depicted in Fig. 2. Moreover, edge servers exploit their idle times to proactively render and cache the HD frames of users affected by the popular impulse actions, such that the computing latency is minimized. Finally, it is assumed that a low quality (LQ) version of the video frame, with data size $L_{fu}^{\text{LQ}} \ll L_{fu}^{\text{HD}}$, can be processed locally in the mmHMD to ensure smooth game play if the HD video frame cannot be delivered on time.

B. mmWave Communication Model

The mmWave channel is based on measurement results of LOS and NLOS paths for the 60-GHz indoor channels [10], and includes both pathloss attenuation l_{au} and small Nakagami fading with coefficient $g_{au}(t)$. The channel gain h_{au} from mmAP a to mmHMD in VRP p is thus given by $|h_{au}(t)|^2 = l_{au}|g_{au}(t)|^2$.

The pathloss ℓ_{au} is considered LOS when $\nexists \text{ VRP } u' \in \mathcal{U} \setminus u$ such that the area defined by the d -diameter circle associated to its head+mmHMD intercepts the ray traced from mmAP a to mmHMD receiver of VRP u ; the path is considered NLOS otherwise⁴. Neither external interference leakage into the finite area of the arcade nor reflections due to walls, ceiling or the VRPs themselves are explicitly incorporated in the channel model. They are only accounted for in a coarse way through the different LOS and NLOS parameters. Accordingly, the pathloss exponent α_{au} in l_{au} will take value α_L if the link from mmAP a to the mmHMD receiver u is LOS and value α_N otherwise. Similarly, the corresponding Nakagami shape factor m_{au} will take value m_L for LOS and m_N for NLOS paths; it is further assumed that $g_{au}(t)$ is i.i.d. and not temporally correlated.

For tractability, the radiation pattern of actual directional antennas is approximated with a 2D sectored antenna model [11]. Let $g_{au}^{\text{Tx}}(\varphi_a, \vartheta_{up}^{\text{Tx}}(t))$ and $g_{au}^{\text{Rx}}(\varphi_u, \vartheta_{au}^{\text{Rx}}(t))$ denote the transmission and reception antenna gains from mmAP a to the mmHMD of VRP u as given by

$$g_{au}^{\text{Tx}}(\varphi_a, \vartheta_{au}^{\text{Tx}}(t)) = \begin{cases} \frac{2\pi - (2\pi - \varphi_a)g_{sl}}{\varphi_a}, & |\vartheta_{au}^{\text{Tx}}(t)| \leq \frac{\varphi_a}{2}, \\ g_{sl}, & \text{otherwise,} \end{cases} \quad (1)$$

with $\text{Tx} \in \{\text{Tx, Rx}\}$, and where $\vartheta_{au}^{\text{Tx}}(t)$ stands for the angular deviation from the boresight directions, and g_{sl} is the constant sidelobe gain with $g_{sl} \ll 1$.

High directionality of mmWave communications motivates a search process to find the boresight directions corresponding to the best path between the mmAP and the mmHMD and take full advantage of beamforming gains as per (1). To that end, periodically each of the A mmAPs will sequentially perform

⁴Capturing the blockage arriving from game-engagement related limb movements, e.g. VRPs raising their hands and blocking their own or some other mmWave link is left for future work.

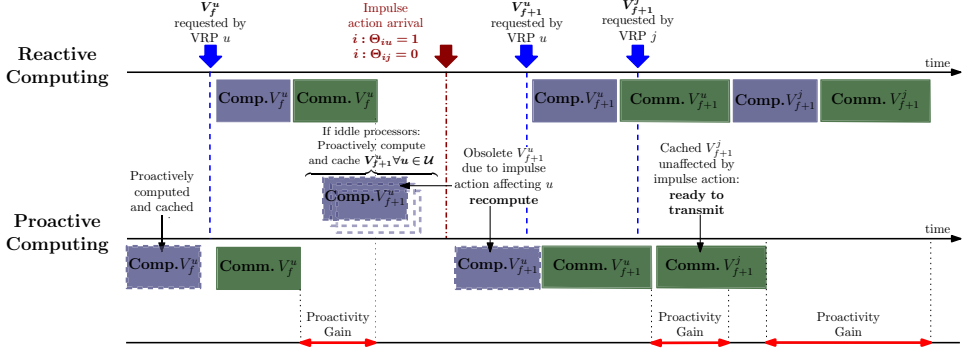


Figure 2. Time dynamics for reactive and proactive computing.

beam training with the $|\mathcal{U}_a|$ VRPs within its coverage area, $\mathcal{U}_a \subset \mathcal{U}$. After the best steerings for all feasible VRPs have been learned, and following a transmission interval level VRP scheduling decision, data transmission begins.

The analog beamformers on the mmAPs and VRPs sides are determined after a two-stage beam training process [12]. Let $\tau = \{\tau_1, \tau_2, \dots, \tau_A\}$ denote the vector of alignment delays for the A mmAPs in the system, then on an *a priori* knowledge of mmAPs fixed location and of VRPs sector⁵, the experienced alignment delay τ_{au} due to beam training is $\tau_{au} = \frac{\psi_a}{\varphi_a} T_p$, where T_p is the pilot symbol transmission time and ψ_a, φ_a denote the sector-level and beam-level beamwidths for mmAP a . The overall alignment delay is $\tau = \sum_{a \in \mathcal{A}} \sum_{u \in \mathcal{U}_a} \tau_{au}$. To overcome vulnerability to channel intermittency due to blockage and misalignment, mmHMDs are assumed to be capable of leveraging MC implemented through coordinated joint transmission of VR player data from multiple mmAPs. An indicator variable $x_{au}(t)$ is therefore defined if mmAP a schedules VRP u at time instant t . The maximum achievable rate (in Gbps) for mmHMD u is given by

$$r_u(t) = (1 - \tau) B \log_2 (1 + \gamma_u(t)), \quad (2)$$

$$\gamma_u(t) = \frac{\sum_{a \in \mathcal{A}} x_{au}(t) p_a |h_{au}(t)|^2 g_{au}^{\text{Tx}}(t) g_{au}^{\text{Rx}}(t)}{\sum_{a' \in \mathcal{A}} (1 - x_{au}(t)) p_{a'u} |h_{a'u}(t)|^2 g_{a'u}^{\text{Tx}}(t) g_{a'u}^{\text{Rx}}(t) + N_0 B}, \quad (3)$$

where the achievable SINR term $\gamma_u(t)$ should, in addition to the effective received power at mmHMD u from mmAPs a : $x_{au}(t) = 1$ and to Gaussian noise, account for the effect of other interfering mmAPs a' : $x_{a'u}(t) = 0$ through channel and antenna gains, $|h_{a'u}(t)|^2$ and $g_{a'u}^{\text{Tx}}, g_{a'u}^{\text{Rx}}$ respectively.

C. Computing Model

The total perceived delay to compute and deliver an HD video frame is expressed as:

$$D_{uf}(t) = \xi_{fu}(D_{uf}^{\text{cp}}(t) + D_{uf}^{\text{cm}}(t) + \tau_{\text{EP}}), \quad (4)$$

where ξ_{fu} is a binary function that equals 1 when the HD video frame is delivered to VRP u and equals 0 if the LQ frame is delivered, D_{uf}^{cp} and D_{uf}^{cm} are the computing and communication delays of HD frame f initiated from user u , and τ_{EP} is the processing latency which accounts for

⁵A reasonable assumption due to highly accurate and frequent VRP location tracking and to the slowness of human movement at ms scale.

the edge server processing, storage processing and the UL transmission of user pose and action data. Here, we focus on the effect of computation delay in the edge servers and the DL communication delay, i.e., the access to the backhaul is assumed to be wired. Let the computing delay D_{uf}^{cp} be expressed as follows:

$$D_{uf}^{\text{cp}}(t) = \left(\frac{\kappa L_{fu}^{\text{HD}}}{c_e} + W_{uf}(t) \right) z_{fu}(t) (1 - y_{fu}(t)), \quad (5)$$

where c_e is the computation capability of edge server e , $z_{fu}(t)$ and $y_{fu}(t)$ indicate that the video frame f of user u is scheduled for computing, and is cached in the fog network at time instant t , respectively, and W_{uf} is the computation waiting time of HD frame f of user u in the service queue, defined as $Q(t)$. Furthermore, Let the communications delay D_{uf}^{cm} be as follows:

$$D_{uf}^{\text{cm}}(t) = \arg \min_{d_u} \sum_{t'=D_{uf}^{\text{cp}}(t)+1}^{D_{uf}^{\text{cp}}(t)+d_u} \left(T_t r_u(t') \geq L_{fu}^{\text{HD}} \right), \quad (6)$$

where the $\arg \min$ function is to find the minimum number of time slots needed for the video frame f to be delivered.

The objective of the proposed approach is to maximize the HD video frame delivery $\xi = [\xi_{fu}]$ subject to latency constraints. The optimization variables are the scheduling, caching, and computing matrices, expressed as $\mathbf{X}(t) = [x_{ua}(t)]$, $\mathbf{Y}(t) = [y_{fu}(t)]$, and $\mathbf{Z}(t) = [z_{fu}(t)]$ respectively. The optimization problem is cast as follows:

$$\max_{\mathbf{X}(t), \mathbf{Y}(t), \mathbf{Z}(t)} \sum_{u=1}^U \sum_{f=1}^F \xi_{fu} \quad (7a)$$

$$\text{subject to } \Pr(D_{uf}(t) \geq D_{\text{th}}) \leq \epsilon, \forall f \in \mathcal{F}, \forall u \in \mathcal{U}, \quad (7b)$$

$$\sum_{u=1}^U x_{ua}(t) \leq 1, \forall a \in \mathcal{A}, \quad (7c)$$

$$\sum_{u=1}^U \sum_{f=1}^F y_{fu}(t) \leq S, \quad (7d)$$

$$\sum_{u=1}^U \sum_{f=1}^F z_{fu}(t) \leq E, \quad (7e)$$

where (7b) is a probabilistic delay constraint that ensures the communication latency is bounded by a threshold value D_{th} with a probability $1 - \epsilon$. Constraint (7c) ensures that

Algorithm 1 Joint computing and caching algorithm.

- 1: **Implementation at each time instant t :**
- 2: **Repeat** find $v =$ vacant cloudlet
- Priority one: real-time scheduling**
- 3: find u where $V_f^u(t)$ is not computed
- 4: $v \rightarrow \text{allocated}$, $z_{fu}(t) \rightarrow 1$
- Priority two: predictive computing and caching**
- 5: Find u and t' where $t' \in (t : t + T_w)$ and $V_f^u(t')$ is not computed
- 6: $v \rightarrow \text{allocated}$, $z_{fu}(t) \rightarrow 1$
- 7: compute and cache $V_f^u(t')$
- Priority three: predictive impulse computing and caching**
- 8: Sort \mathcal{I} by popularity
- 9: **Repeat** Select i as the most popular \mathcal{I}
- 10: find $u: \theta_{u,i} = 1$
- 11: $v \rightarrow \text{allocated}$, $z_{fu}(t) \rightarrow 1$
- 12: compute and cache $V_f^u(t+1)$
- 13: **Until** at least one of the following conditions is true
 - no vacant cloudlets
 - cache is full
 - upcoming frames of impacted users from all \mathcal{I} are computed

mmAP serves one VRP at a time. (7d) limits the number of cached frames to a maximum of S . Constraint (7e) is over the maximum number of simultaneous computing processes. The above problem is a combinatorial problem with non-convex cost function and probabilistic constraints, for which finding an optimal solution is computationally complex [13]. The non-convexity is due to the interference from other mmAPs in the rate term in the delay equation. To make the problem tractable, we use the Markov's inequality to convert the probabilistic constraint in (7b) to a linear constraint [13] expressed as $\mathbb{E}\{D_{uf}(t)\} \leq D_{\text{th}}\epsilon$. Hence, it can be rewritten as:

$$\mathbb{E}\{D_{uf}^{\text{cp}}(t) + D_{uf}^{\text{cm}}(t)\} = \mathbb{E}\{D_{uf}^{\text{cp}}(t)\} + \mathbb{E}\{D_{uf}^{\text{cm}}(t)\} \leq D_{\text{th}}\epsilon \quad (8)$$

The above expectation is hard to calculate due to having the $\arg \min$ function in the $D_{uf}^{\text{cm}}(t)$. Therefore, we express the second expectation as $\mathbb{E}\{D_{uf}^{\text{cm}}(t)\} = \frac{L_{fu}^{\text{HD}}}{T_t \bar{r}_u(t)}$, where $\bar{r}_u(t)$ is the time-average service rate of VRP u from mmAP p at time instant t , expressed as $\bar{r}_u(t) = \sum_{\tau=1}^t r_a(\tau)$. Hence, the ultra-reliable low latency communication (URLLC) constraint can be rewritten as:

$$\frac{L_{fu}^{\text{HD}}}{T_t \bar{r}_u(t)} + \frac{\kappa L_{fu}^{\text{HD}}}{c_e} + \mathbb{E}\{W_{uf}(t)\} \leq D_{\text{th}}\epsilon. \quad (9)$$

Similarly, the average waiting time can be expressed as $\mathbb{E}\{W_{uf}(t)\} = \sum_{i|V_f^i \in Q(t)} \frac{L_{fi}^{\text{HD}}}{T_t \bar{r}_i(t)}$, and (9) rewritten as:

$$\frac{L_{fu}^{\text{HD}}}{T_t \bar{r}_u(t)} \leq D_{\text{th}}\epsilon - \sum_{V_f^i \in Q(t)} \frac{L_{fi}^{\text{HD}}}{T_t \bar{r}_i(t)} - \frac{\kappa L_{fu}^{\text{HD}}}{c_e}. \quad (10)$$

The average rate $\bar{r}_u(t)$ can be separated into the instantaneous time rate at time instant t and the average rate in the previous time instants (that can be estimated), i.e., $\bar{r}_u(t) = \sum_{\varrho=1}^t r_u(\varrho) = r_u(t) + \sum_{\varrho=1}^{t-1} r_u(\varrho)$. In other words, to reach the desired latency requirement, a maximum value of $\frac{L_{fu}^{\text{HD}}}{T_t \bar{r}_u(t)}$ that satisfies the above formula should be guaranteed to admit admitted a request to an mmAP.

Next, a joint VRP-mmAP matching and scheduling scheme is proposed to solve the optimization problem in (7).

Algorithm 2 VRP-mmAP matching algorithm.

- 1: **Initialization:** all players and mmAPs start unmatched.
- 2: Each mmAP constructs its preference list as per (12)
- 3: Each player constructs its preference list as per (13)
- 4: **repeat** an unmatched player u , i.e., $\Upsilon(u) = \phi$ proposes to its most preferred mmAP a that satisfies $a \succ_u u$
 - 5: **if** $\Upsilon(a) = \phi$, $\%$ Not yet matched
 - 6: $\Upsilon(a) = u$, $\Upsilon(u) = a$, $\%$ player u proposal is accepted
 - 7: **else** $\%$ Matched to $u' \rightarrow \Upsilon(a) = u'$,
 - 8: **if** $u' \succ_a u$ $\%$ player u proposal is rejected
 - 9: player u removes mmAP a from its preference list
 - 10: **else** $\%$ player u proposal is accepted
 - 11: $\Upsilon(a) = u, \Upsilon(u) = a, \Upsilon(u') = \phi$
 - 12: player u' removes mmAP a from its preference list
 - 13: **end if**
 - 14: **end if**
 - 15: **if** $\gamma_u < \gamma^{\text{Th}}$
 - 16: split u into two players u_1 and u_2 , $\Upsilon(u_2) = \phi$
 - 17: **end if**
 - 18: **until** all players are either matched with $\gamma_u \geq \gamma^{\text{Th}}$ or not having mmAPs that satisfy $a \succ_u u$ in their preference lists
 - 19: **Output:** a stable matching Υ

III. JOINT PROACTIVE COMPUTING AND MATCHING

As stated above, the optimization problem in (7) is computationally hard to solve. We rather decouple it into two subproblems of computation scheduling and VRP association.

A. Computing and Caching Scheme

During the game play, the edge computing network minimizes the computing service delay by leveraging the pose prediction of users to proactively compute their HD video frames as well as caching the updated HD video frames resulting from randomly arriving impulse actions. In the case that impulse action arrives in which the corresponding frames for the affected users are not computed, the real time computing is giving the highest priority. Therefore, we propose a three priority level algorithm to schedule HD frame computing of users. The detailed algorithm is described in Algorithm 1.

B. Player-Server Matching

Our next step is to propose a VRP-mmAP association scheme that solves the constrained minimization problem in (7). The association problem is formulated as a matching game [14] between the mmAPs and the VRPs. In this game, VRPs seek to maximize their VR experience by competing for mmWave time slots from different mmAPs. Whenever a player in the network requests a new HD frame, a new set of matching pairs is found using the proposed approach. The matching game consists of a two sets of players and mmAPs, where each member of one set has a preference profile over the members of the other sets. Preferences of mmAPs and players are denoted by \succ_a and \succ_u , and reflect how each member of a set ranks the members of the other set.

Definition 1. Given two disjoint sets of mmAPs and players $(\mathcal{A}, \mathcal{U})$, a *matching* is defined as a *one-to-one* mapping Υ from the set $\mathcal{E} \cup \mathcal{U}$ into the set of all subsets of $\mathcal{A} \cup \mathcal{U}$, such that for each $a \in \mathcal{A}$ and $u \in \mathcal{U}$:

- 1) $\forall u \in \mathcal{U}, \Upsilon(u) \in \mathcal{A} \cup u$, where $\Upsilon(u) = u$ means that a player is not associated to a remote server, and will perform local LQ frame processing.

- 2) $\forall a \in \mathcal{A}, \Upsilon(a) \in \mathcal{U} \cup \{a\}$, where $\Upsilon(a) = a$ means that the mmAP a have no associated players.
- 3) $|\Upsilon(u)| = 1, |\Upsilon(a)| = 1; 4) \Upsilon(u) = a \Leftrightarrow \Upsilon(a) = u$.

By inspecting the problem in (7), we can see that the one-to-one mapping of the matching game satisfies the constraint (7c). Moreover, since preference profiles can be defined to capture the cost function of the matching sets. The utility of the mmAPs will essentially reflect the latency constraint in (10). Therefore, we define the utility of associating player u to mmAP a as:

$$\Phi_{au}(t) = D_{\text{th}}\epsilon - \sum_{i|V_f^i \in Q(t)} \frac{L_{fi}^{\text{HD}}}{T_t \bar{r}_i(t)} - \frac{\kappa L_{fu}^{\text{HD}}}{c_e} - \frac{L_{fu}^{\text{HD}}}{T_t \bar{r}_u(t)}, \quad (11)$$

and the mmAP preference as:

$$u \succ_a u' \Leftrightarrow \Phi_{au}(t) > \Phi_{au'}(t), \quad a \succ_a u \Leftrightarrow \Phi_{au}(t) < 0, \quad (12)$$

where the second preference states that a mmAP is not interested in matching to a player that will violate its latency constraint. In other words, the utility of each cloudlet is to seek a matching that maximizes the difference between the right hand side and the left hand side of the inequality in (10), such that the constraint is met as a stable matching is reached. To meet the players' reliability target, we define the preference profiles of the players as to maximize their link quality as follows:

$$a \succ_u a' \Leftrightarrow |h_{au}(t)|^2 g_{au}^{\text{Tx}}(t) g_{au}^{\text{Rx}}(t) < |h_{a'u}(t)|^2 g_{a'u}^{\text{Tx}}(t) g_{a'u}^{\text{Rx}}(t) \quad (13)$$

Since users may not always find a single reliable link, we propose to split the users that are matched but with an SINR below a predefined threshold γ^{Th} into multiple players, allowing to be matched to multiple mmAPs and satisfy their link reliability requirements subject to mmAP availability.

Next, matching stability is defined and an efficient multi-stage algorithm based on deferred-acceptance (DA)[15] to solve it.

Definition 2. Given a matching Υ with $\Upsilon(a) = u$ and $\Upsilon(u) = a$, and a pair (u', a') with $\Upsilon(a) \neq u'$ and $\Upsilon(u) \neq a'$, (u', a') is said to be blocking the matching Υ and form a blocking pair if: 1) $u' \succ_a u$, 2) $a' \succ_u a$. A matching Υ^* is stable if there is no blocking pair.

Remark 1. The algorithm described in Algorithm 2, converges to a two-sided stable matching of players to mmAPs or to their local servers [15].

IV. SIMULATION RESULTS

In this section, we numerically validate the effectiveness of the proposed solution. We also compare the proposed approach against two benchmarking schemes:

- 1) *Baseline 1*, with neither MC nor proactive computing and caching. Requests are computed in real time after they are initiated, and are transmitted through single-connectivity links.
- 2) *Baseline 2*, without MC, but assumes proactive computing and caching capabilities.

We consider a gaming arcade with a capacity of 8x8 VR pods and a set of default parameters⁶ unless stated otherwise.

⁶We consider 100 impulse actions with popularity parameter $z = 0.8$, a uniformly distributed impact matrix θ , $D_{\text{th}} = 100$ ms $\epsilon = 0.1$, 10 dBm mmAP transmit power, $L_f^{\text{HD}} = \sim \exp(2)$ Gbit, $\kappa/c_e = 5 * 10^{-8}$, $S/A = 20$ video frames, and $T_w = 100$ ms.

Impulse actions arrive following the Zipf popularity model of parameter z [16]. Accordingly, the arrival rate for the i^{th} most popular action is proportional to $1/i^z$.

A. Impact of number of players

First, we investigate the performance of the proposed approach when the number of players increases. We fix the number of mmAPs and servers to 16. In Fig. 3, we show the 90th percentile communication delay (D_{uf}^{cm} 90 pctl) for different schemes, which increases with the network density. This is due to the increase in offered load, as compared to the network capacity, and the higher levels of interference. As the number of players increases, the proposed approach achieves up to 25% reduction in the D_{uf}^{cm} 90 pctl, due to the MC gain that allows users with weak links to receive from multiple servers. In Fig. 4, we show the change in both average computing and communication delay. For the computing part, both the proposed approach and Baseline 2 achieve significant reduction in the computing delay, due to leveraging the proactivity to cut down the rendering latency. The proposed approach further minimizes the latency due to enabling MC in dense network conditions associated with high interference/blockage levels.

B. Impact of number of mmAPs

Next, we investigate the performance of the proposed approach as the number of mmAPs increases, while fixing the number of players to the maximum arcade capacity of 64. We assume the number of servers in the fog network also matches the number of mmAPs. First, Fig. 5 shows the D_{uf}^{cm} 90 pctl performance. Intuitively, low number of servers will incur higher delay due to having higher offered load than what the mmAPs can serve. However, we observe that in different mmAPs/servers density, the D_{uf}^{cm} 90 pctl is halved using the proposed approach. Finally, Fig. 6, shows the computing and communication delay performance. We can see that, at low number of servers, the computing delay is always high, due to not having enough computing resources to serve the high number of players. The network can hardly serve the real-time computing requests, leaving no room for proactive computing. Accordingly, higher number of servers are needed to achieve proactive computing gains. However, communication delay can be reduced by up to 30% at low number of mmAPs.

V. CONCLUSIONS

In this paper, we have studied the problem of ultra-reliable and low latency wireless VR networks. A joint proactive computing and user association scheme is proposed in mmWave enabled VR for interactive gaming. In the proposed scheme, information about the game players' upcoming pose and game action is leveraged to proactively render their HD video frames such that computing latency is minimized. To ensure reliable and low latency communication, a matching algorithm has been proposed to associate players to mmAPs and enable multi-connectivity, in which multiple mmAPs jointly transmit the video frames to players to overcome the effect of channel variability. Simulation results have shown that the proposed scheme achieves significant reduction in both computing and

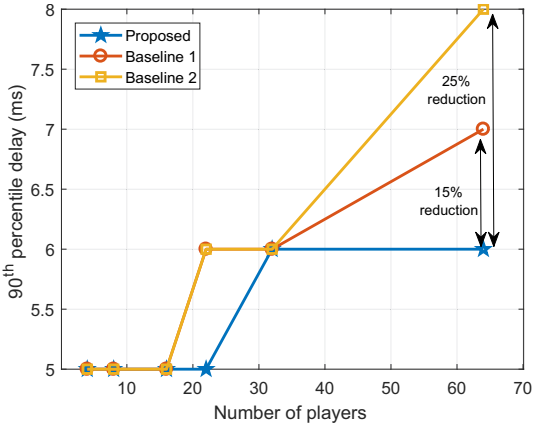


Figure 3. 90th percentile communication delay versus number of users, for 16 mmAPs.

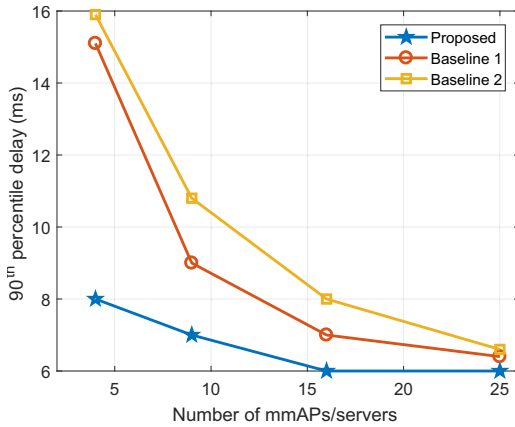


Figure 5. 90th percentile communication delay versus number of servers, for 64 players.

communication latency under different network conditions, as compared to different baseline schemes.

VI. ACKNOWLEDGMENTS

This research was partially supported by the Academy of Finland project CARMA, the NOKIA donation project FOGGY and by the Spanish MINECO under grant TEC2016-80090-C2-2-R (5RANVIR).

REFERENCES

- [1] E. Baştuğ, M. Bennis, M. Médard *et al.*, “Toward Interconnected Virtual Reality: Opportunities, Challenges, and Enablers,” *IEEE Commun. Mag.*, vol. 55, no. 6, pp. 110–117, June 2017.
- [2] M. S. ElBamby, C. Perfecto, M. Bennis *et al.*, “Towards low-latency and ultra-reliable virtual reality,” *IEEE Network*, 2017, to appear.
- [3] F. Qian, L. Ji, B. Han *et al.*, “Optimizing 360° video delivery over cellular networks,” in *Proc. Int. Conf. Mobile Comp. and Networking (Mobicom)*, New York, NY, USA, 2016, pp. 1–6.
- [4] R. Ju, J. He, F. Sun *et al.*, “Ultra Wide View Based Panoramic VR Streaming,” in *Proc. ACM SIGCOMM Workshop on Virtual Reality and Augmented Reality Network (VR/AR Network)*, 2017.
- [5] K. Doppler, E. Torkildson, and J. Bouwen, “On Wireless Networks for the Era of Mixed Reality,” in *Proc. Eur. Conf. on Networks and Commun. (EuCNC)*, June 2017, pp. 1–6.
- [6] M. Chen, W. Saad, and C. Yin, “Virtual reality over wireless networks: Quality-of-service model and learning-based resource management,” *CoRR*, vol. abs/1703.04209, 2017.
- [7] F. Bonomi, R. Milito, J. Zhu *et al.*, “Fog computing and its role in the internet of things,” in *Proc. 1st Edition of the MCC Workshop on Mobile Cloud Computing*, ser. MCC ’12, 2012, pp. 13–16.
- [8] M. S. Elbamby, M. Bennis, and W. Saad, “Proactive edge computing in latency-constrained fog networks,” in *Proc. Eur. Conf. on Networks and Commun. (EuCNC)*, June 2017, pp. 1–6.
- [9] Y. Mao, C. You, J. Zhang *et al.*, “A survey on mobile edge computing: The communication perspective,” *IEEE Commun. Surveys Tuts.*, vol. PP, no. 99, pp. 1–1, Aug. 2017.
- [10] H. Xu, V. Kukshya, and T. S. Rappaport, “Spatial and temporal characteristics of 60-GHz indoor channels,” *IEEE J. Sel. Areas Commun.*, vol. 20, no. 3, pp. 620–630, Apr. 2002.
- [11] J. Wildman, P. H. J. Nardelli, M. Latvala-aho *et al.*, “On the joint impact of beamwidth and orientation error on throughput in directional wireless poisson networks,” *IEEE Trans. Wireless Commun.*, vol. 13, no. 12, pp. 7072–7085, Dec. 2014.
- [12] J. Wang, Z. Lan, C.-W. Pyu *et al.*, “Beam codebook based beamforming protocol for multi-Gbps millimeter-wave WPAN systems,” *IEEE J. Sel. Areas Commun.*, vol. 27, no. 8, pp. 1390–1399, Oct 2009.
- [13] A. Mukherjee, “Queue-aware dynamic on/off switching of small cells in dense heterogeneous networks,” in *IEEE Globecom Workshops (GC Wkshps)*, Dec. 2013, pp. 182–187.
- [14] O. Semiari, W. Saad, S. Valentin *et al.*, “Matching theory for priority-based cell association in the downlink of wireless small cell networks,” in *2014 IEEE Int. Conf. on Acoustics, Speech and Signal Processing (ICASSP)*, May 2014, pp. 444–448.
- [15] A. Roth and M. Sotomayor, “Two-sided matching: A study in game-theoretic modeling and analysis,” *Cambridge University Press*, 1992.
- [16] E. Baştuğ, M. Bennis, and M. Debbah, “Living on the edge: The role of proactive caching in 5G wireless networks,” *IEEE Commun. Mag.*, vol. 52, no. 8, pp. 82–89, Aug. 2014.

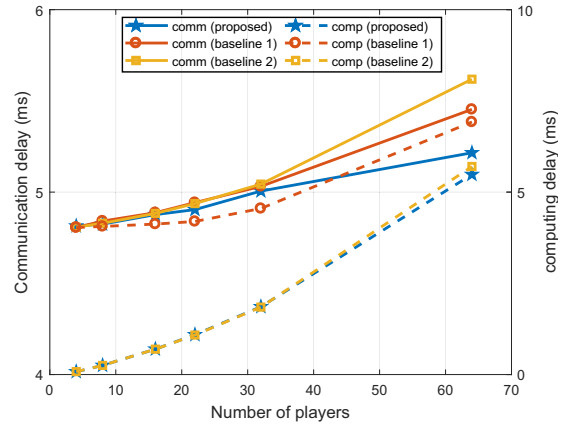


Figure 4. Average communication delay (solid lines) and computing delay (dashed lines) versus number of users, for 16 mmAPs.

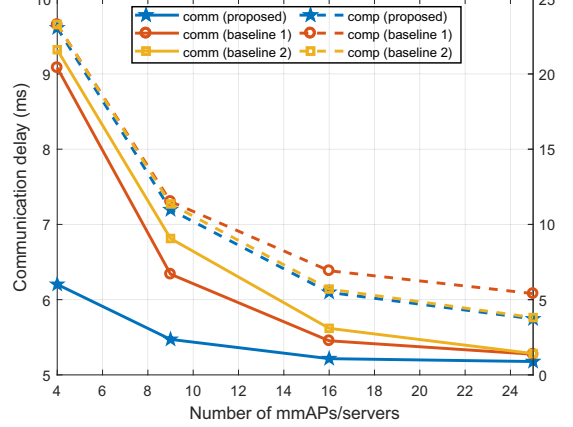


Figure 6. Average communication delay (solid lines) and computing delay (dashed lines) versus number of servers, for 64 players.